Concurrent Optical and Magnetic Resonance Microscopy

Frederik Testud[1], Elmar Fischer[1], Katharina Göbel[1], Nils Spengler[2], Ulrike Wallrabe[2], Maxim Zaitsev[1], and Matthias Wapler[2]
[1]*Medical Physics, University Medical Center Freiburg, Freiburg, Germany,* [2]*Department for Microsystems Engineering – IMTEK, University of Freiburg, Freiburg, Germany*

Introduction Magnetic Resonance (MR) microscopy is a method for high-resolution imaging resolving structures smaller than 100 µm [1,2]. However, despite technical improvements of MR imaging, a lack of understanding remains regarding the effect of pathologies on a cellular level and their relations to MR contrast changes on a macroscopic level. The identification of specific microstructural elements is therefore done by light-microscopy based correlative histology techniques [3]. MR image artefacts because of susceptibility effects, motion or sample preparation during staining can lead to discrepancies, impairing the comparison between images from both modalities. In order to overcome these limitations, an Optical Microscope (OM) is proposed, which can be placed inside the bore of an ultra-high field small animal MR scanner and allow to concurrently perform optical microscopy and MR imaging of the sample without compromises in the optical resolution. Here we present the design of the OM and initial proof-of-concepts results acquired from Organotypic Hippocampal Slice Cultures (OHSC).

Methods The OM setup (Fig. 1) was custom-built to fit inside a quadrature Radio Frequency (RF) coil (∅ = 72 mm, Bruker Biospin, Ettlingen, Germany), which is used for transmit and receive, of a 9.4 T small animal scanner (94/20, AVIII, Bruker Biospin). The microscope optic is inside the RF coil (Fig. 2) and arranged such that the optical Field-Of-View (oFOV) is in the isocentre of the magnet. The main direction of observation is anterior-posterior and the optic is designed to provide a distortion-free (apochromatic, diffraction-limited) image throughout the oFOV of 2 mm diameter. The light sources consist of four Red Green Blue White (RGBW) LEDs (Cree XLamp XM-L Color, Cree Inc., Durham, NC, USA). Each LED can be individually controlled to use reflected or transmitted light for bright or dark field microscopy, respectively. A camera (Stingray F-125B, Allied Vision Technologies GmbH, Stadtroda, Germany) with a resolution of 1292×964 px was used to observe the sample concurrently to MR experiments. The camera was electromagnetically shielded by a thin tin-plated copper layer (Fig. 3). The tube in front of the camera contains the part of the optic that projects onto the camera (Fig. 2) and acts as a wave guide to suppress electromagnetic waves penetration (Fig. 3). The RF-noise impact of the OM on MR experiments was estimated by comparing two MR images (RF and gradients turned 'off') acquired with the OM turned 'on' and 'off', respectively. The acquisition bandwidth was set to 200 kHz and 2048 points were acquired in the readout direction. A t-test with a significance level of 0.5 % was performed on the RF- noise data. A field map was acquired with a double echo 3D gradient echo sequence (repetition time TR = 0.5 s, 6 averages, echo time TE1 = 1.5 ms and TE2 = 5.2 ms, matrix size = 128×128×16, FOV = 2.56×2.56×0.32 mm³) and fitted within the oFOV (cylinder with ∅ = 2 mm, 1.6 mm height) to a spherical harmonic expansion up to seventh order [5] to assess local magnetic field distortions. Imaging experiments were performed on an *ex-vivo* OHSC (1×2×0.4 mm³) with a 3D Turbo Rapid Acquisition with Relaxation Enhancement (RARE) sequence (TR = 2 s, TE = 34 ms, matrix size 256×256×32, RARE factor=16, 40 averages, isotropic resolution 94 µm).

Results The mean magnetic field distortion in the optical imaging region was 54 ppb with a root-mean-square inhomogeneity of 14 ppb. A small RF-noise increase of 0.6 % was observed when the OM is turned 'on'. The MR and OM images, acquired simultaneously in the same experiment, are shown in Fig. 4 and 5, respectively. The MR image was interpolated to distinguish anatomical structures. A resolution of the order of microns enabling the identification of hippocampal substructures could be reached with the OM without being altered by the concurrent MR acquisition. The hilus and the granule cell layer can be clearly identified in both images.

Discussion A comparison of the obtained MR and OM images (Fig. 4 and Fig. 5) shows that similar structures can be identified. The combination of both methods can set the framework for an *in vitro* system, which would serve as a basis for a broad spectrum of new experiments, providing deeper insights into physiological processes. In near future, a local surface receive micro-coil in form of a Helmholtz coil pair [6] will be integrated to the OM to allow for state-of-the-art MR microscopy measurements. Also an adaptive lens [7] will be mounted to the OM to flexibly vary the focus.

Conclusion An MR-compatible optical microscope is presented for an ultra-high field small animal scanner and a first *ex-vivo* experiment is shown. The OM creates a negligible demagnetization field in the region of the sample and a minor RF-noise increase, which do not impact MR imaging. Additionally, optical microscopy was not affected by concurrent MR experiments.

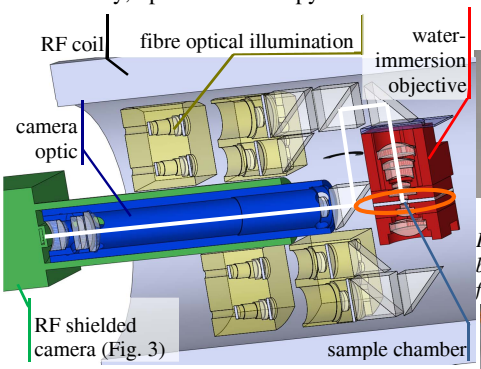

Fig. 2: Schematic overview of the microscope and the camera optic inside the RF coil. The sample chamber is in the centre of the oFOV (orange ellipsoid). Optical and support materials of the OM close to the oFOV were chosen [4] such to create a susceptibility matched environment for the sample. The white line depicts the optical path of the sample projection to the camera.

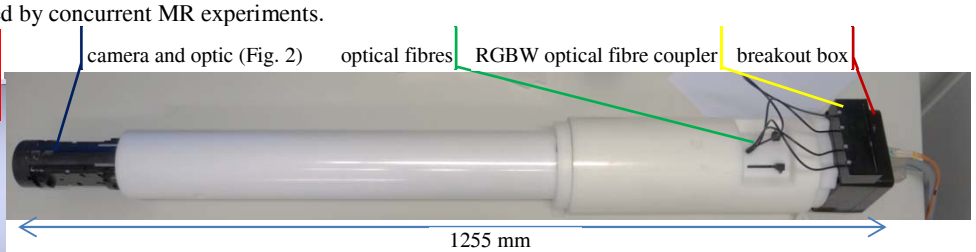

Fig. 1: Photo of the microscope assembly. Four RGBW LEDs are located in the optical fibre coupler. The breakout box provides the power supply and the connection to the camera and the power supply to the optical fibre coupler. The camera and the optic are inside the quadrature coil during the MR experiments.

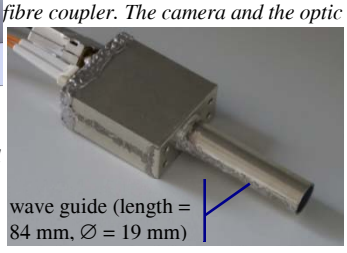

Fig. 3: RF-shielded camera (dimensions: 67×56.2×28.2 mm³).

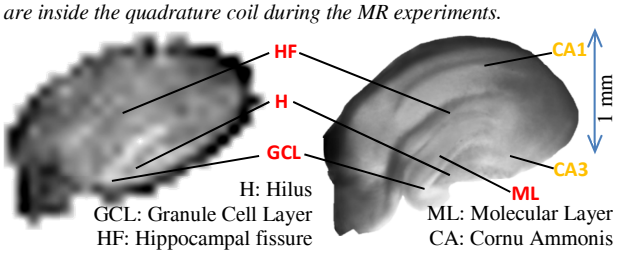

Fig. 4: Masked and interpolated OHSC MR image.

Fig. 5: Masked OHSC OM image using bright field illumination.

References [1]Aguayo et al., Nature, 322:1986; [2] Flint et al., NI, 60:2012; [3] Meadowcroft et al., MRM, 57:2007; [4] Wapler et al., JMR, 242:2014; [5] Testud et al., Proc ISMRM, 2009; [6] Spengler et al., J Micromech Microeng 24:2014; [7] Wapler et al., Proc. ISOT, 2014;

Acknowledgments This research was funded by the Baden-Württemberg Stiftung through the project 'ADOPT-TOMO' and in part by the 'BrainLinks-BrainTools' Cluster of Excellence of the German Research Foundation, grant #EXC 1086.